Biochimica et Biophysica Acta 1804 (2010) 1925–1936

Contents lists available at ScienceDirect

Biochimica et Biophysica Acta

journal homepage: www.elsevier.com/locate/bbapap

Molecular identification of unsaturated uronate reductase prerequisite for alginate metabolism in *Sphingomonas* sp. A1

Ryuichi Takase [a], Akihito Ochiai [a], Bunzo Mikami [b], Wataru Hashimoto [a], Kousaku Murata [a,*]

[a] Laboratory of Basic and Applied Molecular Biotechnology, Graduate School of Agriculture, Kyoto University, Uji, Kyoto 611-0011, Japan
[b] Laboratory of Applied Structural Biology, Graduate School of Agriculture, Kyoto University, Uji, Kyoto, Japan

ARTICLE INFO

Article history:
Received 10 April 2010
Received in revised form 11 May 2010
Accepted 19 May 2010
Available online 27 May 2010

Keywords:
Alginate
Crystal structure
2-Keto-3-deoxy-D-gluconic acid
Short-chain dehydrogenase/reductase
Sphingomonas

ABSTRACT

In *Sphingomonas* sp. A1, alginate is degraded by alginate lyases to its constituent monosaccharides, which are nonenzymatically converted to an α-keto acid, namely, 4-deoxy-L-erythro-5-hexoseulose uronic acid (DEH). The properties of the DEH-metabolizing enzyme and its gene in strain A1 were characterized. In the presence of alginate, strain A1 cells inducibly produced an NADPH-dependent DEH reductase (A1-R) in their cytoplasm. Molecular cloning of the enzyme gene indicated that A1-R belonged to the short-chain dehydrogenase/reductase superfamily and catalyzed the conversion of DEH to 2-keto-3-deoxy-D-gluconic acid most efficiently at around pH 7.0 and 50 °C. Crystal structures of A1-R and its complex with NADP were determined at around 1.6 Å resolution by X-ray crystallography. The enzyme consists of three layers (α/β/α), with a coenzyme-binding Rossmann fold. NADP is surrounded by positively charged residues, and Gly-38 and Arg-39 are crucial for NADP binding. Site-directed mutagenesis studies suggest that Ser-150, Tyr-164, and Lys-168 located around the Rossmann fold constitute the catalytic triad. To our knowledge, this is the first report on molecular cloning and structure determination of a bacterial DEH reductase responsible for alginate metabolism.

1. Introduction

Sphingomonas sp. strain A1 forms a pit-like structure, called a "superchannel," on the cell surface and directly incorporates the macromolecule alginate into the cytoplasm. The mechanism and components involved in the molecular machine are described in our previous paper [1]. The incorporated alginate is then depolymerized into disaccharides, trisaccharides, and tetrasaccharides through the action of three cytoplasmic endotype alginate lyases: A1-I, A1-II, and A1-III [2]. The oligosaccharides thus formed are finally degraded by a cytoplasmic exotype alginate lyase, A1-IV, into monosaccharides, which are then nonenzymatically converted to 4-deoxy-L-erythro-5-hexoseulose uronic acid (DEH) [3] (Fig. 1).

DEH was shown to be converted to 2-keto-3-deoxy-D-gluconic acid (KDG) by a certain reductase [4]. However, the genetic, enzymatic, and structural features of this reductase have not been indicated. Here, we describe the molecular characterization and structural determination of a DEH-specific reductase (A1-R) in strain A1 involved in alginate metabolism.

2. Materials and methods

2.1. Materials

Sodium alginate (polymerization degree, ~650; viscosity, 1000 cP) from *Eisenia bicyclis* and Hydroxylapatite were purchased from Nacalai Tesque, Inc. Silica gel 60/Kieselguhr F_{254} thin-layer chromatography (TLC) plates were obtained from Merck. DEAE-Toyopearl 650 M, Butyl-Toyopearl 650 M, and Butyl-Toyopearl 650 S columns were purchased from Tosoh Corp. HiLoad 26/10 Q Sepharose High Performance, HiLoad 16/60 Superdex 75 pg, HiLoad 16/60 Superdex 200 pg, and Mono Q HR 5/5 columns were from GE Healthcare. Restriction endonucleases and DNA-modifying enzymes were from Toyobo. DEH derived from alginate was prepared by digesting sodium alginate with two purified exotype alginate lyases, namely, A1-IV [3,5] and Atu3025 [6], and then purified using a Amicon Ultra-4 centrifugal filter (Millipore) and Bio-Gel P-2 size-exclusion column chromatography (Bio-Rad Laboratories). The purified DEH was confirmed to be almost homogeneous by TLC. Primers used in this work are listed in Table 1. Other analytical grade chemicals were obtained from commercial sources.

Abbreviations: Strain A1, *Sphingomonas* sp. strain A1; DEH, 4-deoxy-L-erythro-5-hexoseulose uronic acid; KDG, 2-keto-3-deoxy-D-gluconic acid; A1-R, DEH-specific strain A1 reductase; TLC, thin-layer chromatography; KPB, potassium phosphate buffer; LC, liquid chromatography; SDS–PAGE, sodium dodecyl sulfate–polyacrylamide gel electrophoresis; MS, mass spectrometry; ESI, electrospray ionization; NMR, nuclear magnetic resonance; A1-R/NADP, A1-R in complex with NADP; r.m.s.d., root-mean-square deviation; PDB, Protein Data Bank; MALDI-TOF, matrix-assisted laser desorption/ionization time-of-flight; SDR, short-chain dehydrogenase/reductase

* Corresponding author. Tel.: +81 774 38 3766; fax: +81 774 38 3767.
E-mail address: kmurata@kais.kyoto-u.ac.jp (K. Murata).

1570-9639/$ – see front matter © 2010 Elsevier B.V. All rights reserved.
doi:10.1016/j.bbapap.2010.05.010

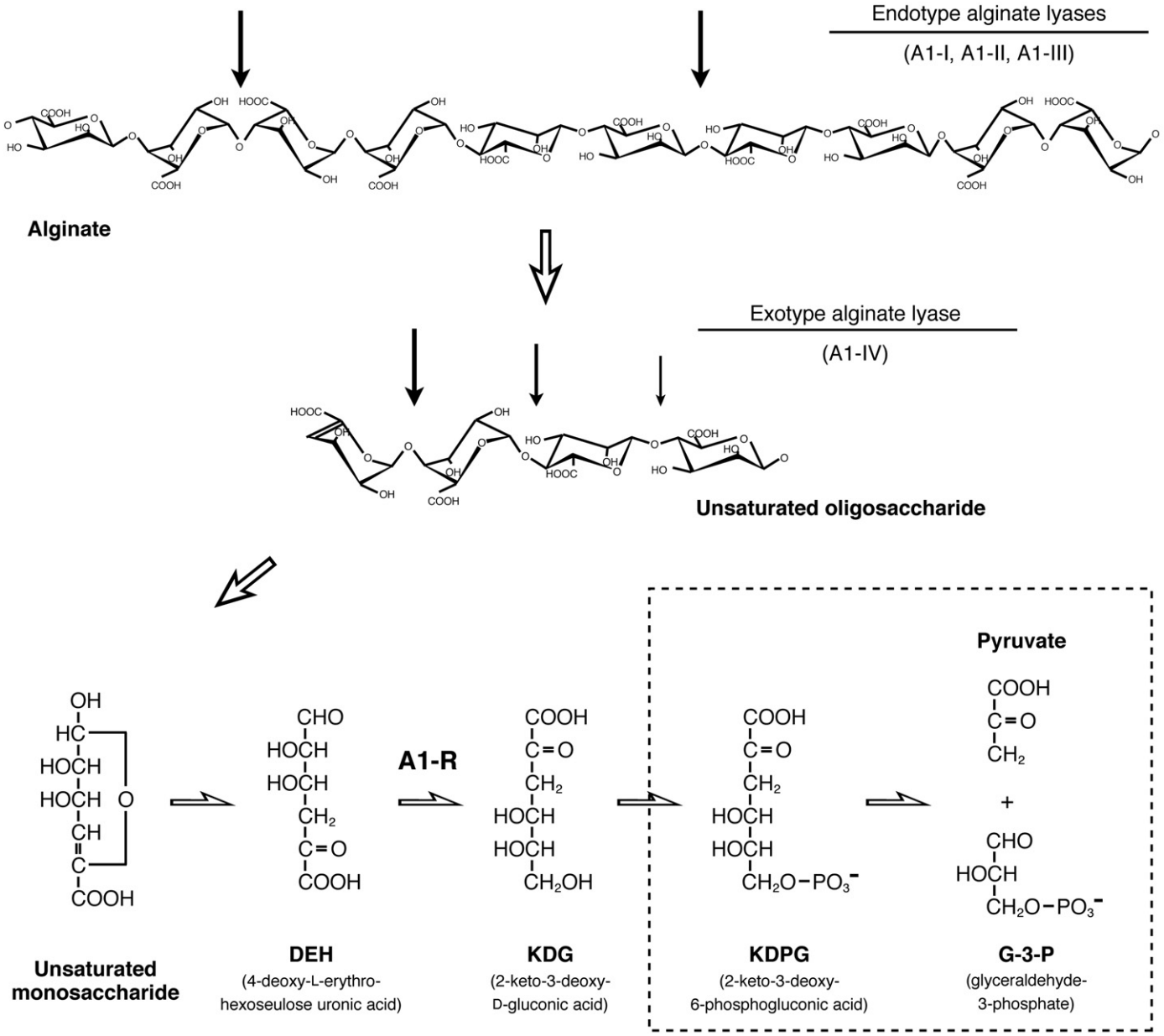

Fig. 1. Alginate metabolic pathway in strain A1. The thick arrows indicate the cleavage sites of each alginate lyase against the substrate. Hypothetical pathways are shown in the dotted frame.

2.2. Microorganisms and culture conditions

Strain A1 cells were routinely cultured at 30 °C in minimal medium containing 5 mg mL^{-1} alginate, 1 mg mL^{-1} $(NH_4)_2SO_4$, 1 mg mL^{-1} KH_2PO_4, 1 mg mL^{-1} Na_2HPO_4, 0.1 mg mL^{-1} yeast extract, and 0.1 mg mL^{-1} $MgSO_4 \cdot 7H_2O$. The cells were also aerobically cultured at 30 °C in minimal medium containing 5 mg mL^{-1} pectin, glucuronic acid, or glucose as the sole carbon source instead of alginate.

As a host for plasmid amplification, *Escherichia coli* strain DH5α (Toyobo) was routinely cultured at 37 °C in LB medium [7] containing ampicillin (100 μg mL^{-1}). *E. coli* strain BL21 (DE3) (Novagen) was used as a host for the overexpression of A1-R. For the expression of A1-R, *E. coli* cells were aerobically cultured at 30 °C in LB medium supplemented with ampicillin (100 μg mL^{-1}). When the turbidity at 600 nm reached 0.6, isopropyl-β-D-thiogalactopyranoside was added to the culture at a final concentration of 0.4 mM, and the cells were further cultured at 16 °C for 42 h.

2.3. Enzymatic and protein assays

The DEH-reducing activity of A1-R was assayed at 30 °C for 5 min in a reaction mixture (0.5 mL) consisting of 1 mM DEH, 0.2 mM NADPH, and 50 mM potassium phosphate buffer (KPB) (pH 7.0). The activity was determined by continuously monitoring the decrease in absorbance at 340 nm, which corresponds to the oxidation of NADPH. One unit (U) of enzymatic activity was defined as the amount of enzyme required to produce 1 μmol of reduced product per min at 30 °C. The protein content was determined according to the procedure of Bradford [8], with bovine serum albumin as the standard.

2.4. Purification of A1-R from strain A1 cells

A1-R was purified from strain A1 cells as follows. Unless otherwise specified, all procedures were performed at 0–4 °C. Cells were grown in 1.5 L of alginate minimal medium (1.5 L per flask), collected by

Table 1
Primers for cloning and site-directed mutagenesis.

Gene or mutant	Oligonucleotides
A1-R_*Nde*I	5′-GGCATATGTTCCCAGACCTCAAAGGCAAGC-3′
A1-R_*Bam*HI	5′-CCGGATCCTCAGTGCTTGTACTGCCCGCC-3′
S150A	5′-GTGATCAGCACCGGGGCGATCGCTGGCCAC-3′
	5′-GTGGCCAGCGATCGCCCCGGTGCTGATCAC-3′
Y164F	5′-CCGGCGCAGGTCTGTTTGGCGCAGCCAAGG-3′
	5′-CCTTGGCTGCGCCAAACAGACCTGCGCCGG-3′
K168A	5′-GGTCTGTATGGCGCAGCCGCGGCTTTCCTGCACAACG-3′
	5′-CGTTGTGCAGGAAAGCCGCGGCTGCGCCATACAGACC-3′
G38D	5′-CCAAGGTCGGCCTGCACGATCGCAAGGCACCCGCC-3′
	5′-GGCGGGTGCCTTGCGATCGTGCAGGCCGACCTTGG-3′
R39I	5′-GGTCGGCCTGCACGGCATCAAGGCACCCGCCAAC-3′
	5′-GTTGGCGGGTGCCTTGATGCCGTGCAGGCCGACC-3′
R39V	5′-GGTCGGCCTGCACGGCGTCAAGGCACCCGCCAAC-3′
	5′-GTTGGCGGGTGCCTTGACGCCGTGCAGGCCGACC-3′
R39W	5′-GGTCGGCCTGCACGGCTGGAAGGCACCCGCCAAC-3′
	5′-GTTGGCGGGTGCCTTCCAGCCGTGCAGGCCGACC-3′
A41E	5′-CGGCCGCAAGGAACCCGCCAACATCG-3′
	5′-CGATGTTGGCGGGTTCCTTGCGGCCG-3′
S16Y	5′-GCGTTCTGATCACCGGTTCGTATCAGGGCATTGGC-3′
	5′-GCCAATGCCCTGATACGAACCGGTGATCAGAACGC-3′
G38E	5′-CCAAGGTCGGCCTGCACGAACGCAAGGCACCCGCC-3′
	5′-GGCGGGTGCCTTGCGTTCGTGCAGGCCGACCTTGG-3′
R39D	5′-GGTCGGCCTGCACGGCGATAAGGCACCCGCCAAC-3′
	5′-GTTGGCGGGTGCCTTATCGCCGTGCAGGCCGACC-3′
G38D/R39D	5′-GGTCGGCCTGCACGATGATAAGGCACCCGCCAACATCG-3′
	5′-CGATGTTGGCGGGTGCCTTATCATCGTGCAGGCCGACC-3′
R39D/K40D	5′-GGTCGGCCTGCACGGCGATGATGCACCCGCCAACATCG-3′
	5′-CGATGTTGGCGGGTGCATCATCGCCGTGCAGGCCGACC-3′
K40D/A41D	5′-CGGCCTGCACGGCCGCGATGATCCCGCCAACATCGATG-3′
	5′-CATCGATGTTGGCGGGATCATCGCGGCCGTGCAGGCCG-3′
G38D/R39E/K40E	5′-GAAGAAGCACCCGCCAACATCGATGAGACCA-3′
	5′-ATCGTGCAGGCCGACCTTGGCGCCT-3′

Single and double underlines indicate restriction and mutation sites, respectively.

centrifugation (6000×*g*, 5 min), and resuspended in 20 mM Tris–HCl (pH 7.5). They were ultrasonically disrupted (Insonator Model 201; Kubota Corp.) at 9 kHz for 20 min, and the clear solution obtained on centrifugation (20,000×*g*, 20 min) was used as the cell-free extract. The extract was applied to a DEAE-Toyopearl 650 M column (2.5 cm×10 cm) previously equilibrated with 20 mM Tris–HCl (pH 7.5). The absorbed proteins were eluted with a linear gradient of NaCl (0–500 mM) in 20 mM Tris–HCl (pH 7.5; 200 mL), with a 1-mL fraction collected every minute. The A1-R active fractions, eluted with 100–200 mM NaCl, were combined and dialyzed for 3 h against 20 mM Tris–HCl (pH 7.5). The dialysate was applied to a HiLoad 26/10 Q Sepharose High Performance column (2.6 cm×10 cm) previously equilibrated with 20 mM Tris–HCl (pH 7.5). These absorbed proteins were eluted with a linear gradient of NaCl (0–1 M) in 20 mM Tris–HCl (pH 7.5; 250 mL), with a 3-mL fraction collected every 0.5 min. The active fractions, eluted with 200–250 mM NaCl, were combined and applied to a HiLoad 16/60 Superdex 200 pg column (1.6 cm×60 cm) previously equilibrated with 20 mM Tris–HCl (pH 7.5) containing 0.15 M NaCl. A1-R was eluted with the same buffer (120 mL) with a 2-mL fraction collected every 2 min, and the active fractions were combined and dialyzed for 3 h against 5 mM KPB (pH 7.0). The dialysate was applied to a Hydroxylapatite column (1 cm×1.5 cm) previously equilibrated with 5 mM KPB (pH 7.0). The absorbed proteins were eluted with a linear gradient of KPB (5–500 mM; 20 mL), with a 1-mL fraction collected every minute. The active fractions obtained on elution with 50–100 mM KPB were combined and saturated with ammonium sulfate (30%). The enzyme solution was then applied to a Butyl-Toyopearl 650 S column (1 cm×1.5 cm) previously equilibrated with 20 mM Tris–HCl (pH 7.5), containing 30% saturated ammonium sulfate. The absorbed proteins were eluted with a linear gradient of saturated ammonium sulfate (30% to 0%; 20 mL), with a 1-mL fraction collected every minute. The active fractions, eluted with 20–10% saturated ammonium sulfate, were combined and applied to a HiLoad 16/60 Superdex 75 pg column (1.6 cm×60 cm) previously equilibrated with 20 mM Tris–HCl (pH 7.5) containing 0.15 M NaCl. A1-R was eluted with the same buffer (120 mL), with a 1-mL fraction collected every minute, and the active fractions were combined and dialyzed for 3 h against 20 mM Tris–HCl (pH 7.5). The dialysate was applied to a Mono Q HR 5/5 column (0.5 cm×5 cm) previously equilibrated with 20 mM Tris–HCl (pH 7.5). The absorbed proteins were eluted with a linear gradient of NaCl (0–300 mM) in 20 mM Tris–HCl (pH 7.5; 30 mL), with a 1-mL fraction collected every minute. The active fractions obtained on elution with 200–250 mM NaCl were combined and dialyzed at 4 °C overnight against 20 mM Tris–HCl (pH 7.5). This dialysate was used as the purified enzyme source (A1-R).

2.5. Liquid chromatography/tandem mass spectrometry (LC-MS/MS)

Protein identification by MS was performed as described elsewhere [9]. Briefly, A1-R resolved on sodium dodecyl sulfate–polyacrylamide gel electrophoresis (SDS–PAGE) was excised and digested with trypsin at 37 °C overnight. The generated peptides were investigated by determining the molecular masses by LC-MS/MS analysis. Paradigm MS-4 (Michrom BioResources) with reversed-phase column chromatography (Magic C18, Michrom BioResources) was used for the LC analysis. The sample was injected into the column at a flow rate of 1 μL min^{-1} for mobile phase buffer A. The chromatography was developed with a 50-min linear gradient from 5% to 65% for buffer B. Buffer A consisted of 2% acetonitrile, 0.1% formic acid, and 0.1% trifluoroacetic acid, and buffer B comprised 90% acetonitrile, 0.1% formic acid, and 0.1% trifluoroacetic acid. Subsequent MS/MS was performed using a LCQ Advantage (Thermo Finnigan) in positive mode with a capillary voltage of 2 kV. For protein identification, the experimentally obtained masses were compared with the theoretical peptide masses, derived from proteins loaded in the strain A1 genome database [10]. The Mascot system [11] was used for the MS/MS ion search.

2.6. Construction of plasmid for overexpression of A1-R and DNA sequencing

The overexpression system for A1-R was constructed in *E. coli* cells as follows. To clone the A1-R gene, PCR was performed in a reaction mixture (100 μL) containing 5 U of KOD polymerase (Toyobo), 0.25 μg of strain A1 genomic DNA, 40 pmol each of forward and reverse primers, 20 nmol of dNTPs, 100 nmol of $MgCl_2$, 5 μL of dimethyl sulfoxide, and the commercial reaction buffer supplied with KOD polymerase. The forward and reverse primers with *Nde*I and *Bam*HI sites (underlined) added to each of their 5′-regions were used for the A1-R gene amplification (Table 1). The PCR conditions were as follows: 94 °C for 30 s, 60 °C for 2 s, and 74 °C for 40 s, for a total of 30 cycles. The PCR products were separated by agarose gel electrophoresis, and the DNA fragment corresponding to the A1-R gene was isolated with a MinElute gel extraction kit (Qiagen). The fragment was ligated with *Hin*cII-digested pUC119 (Takara Bio, Inc.), and the resulting plasmid was digested with *Nde*I and *Bam*HI for isolating the A1-R gene. The *Nde*I–*Bam*HI fragment containing the A1-R gene was then ligated with *Nde*I- and *Bam*HI-digested pET21b (Novagen), yielding pET21b/A1-R. The cloned fragment included the complete sequence of the A1-R gene with the original start and stop codons. Thus, the encoded polypeptide (recombinant A1-R) was not fused to the His-tag encoded by the vector.

The nucleotide sequence of the A1-R gene amplified by PCR was determined by dideoxy chain termination using an automated DNA sequencer (Model 377; Applied Biosystems) [12]. Subcloning,

transformation, and gel electrophoresis were performed as described elsewhere [13].

2.7. Purification of recombinant A1-R from E. coli cells

Unless otherwise specified, all procedures were performed at 0–4 °C. *E. coli* strain BL21 (DE3) cells harboring pET21b/A1-R were grown in 6 L of LB medium (1.5 L per flask), collected by centrifugation (6000×*g*, 5 min), and resuspended in 20 mM Tris–HCl (pH 7.5). The cells were ultrasonically disrupted at 9 kHz for 20 min, and the clear solution obtained on centrifugation (20,000×*g*, 20 min) was used as the cell-free extract. The extract was applied to a DEAE-Toyopearl 650 M column (5.5 cm×20 cm) previously equilibrated with 20 mM Tris–HCl (pH 7.5). The absorbed proteins were eluted with a linear gradient of NaCl (0–700 mM) in 20 mM Tris–HCl (pH 7.5; 1 L), with a 1-mL fraction collected every minute. The active fractions, eluted with 100–200 mM NaCl, were combined and saturated with ammonium sulfate (30%). The enzyme solution was applied to a Butyl-Toyopearl 650 M column (2.5 cm×15 cm) previously equilibrated with 20 mM Tris–HCl (pH 7.5) containing 30% saturated ammonium sulfate. The absorbed proteins were eluted with a linear gradient of saturated ammonium sulfate (30% to 0%; 200 mL), with a 1-mL fraction collected every minute. The active fractions, eluted with 20–10% saturated ammonium sulfate, were combined and dialyzed overnight at 4 °C against 20 mM Tris–HCl (pH 7.5). This dialysate was used as the purified recombinant A1-R.

2.8. Electrospray ionization (ESI)–MS and nuclear magnetic resonance (NMR) spectrometry

Structural determination of the reaction product by recombinant A1-R was carried out as follows. The product was prepared from the reaction mixture of recombinant A1-R and substrate, and purified by gel filtration (Bio-Gel P-2) and normal-phase column chromatography (COSMOSIL HILIC; Nacalai Tesque, Inc.). The LaChrom Elite system (Hitachi), provided with an L-2100 pump (Hitachi), L-2400 UV detector (Hitachi), ERC-3415α on-line degasser (ERC, Inc.), and SmartChrom chromatographic manager (KYA Technologies Corp.) were used for HPLC analysis. The normal-phase column chromatography was developed at a flow rate of 1 mL min^{-1} with an isocratic mobile phase consisting of 30% acetonitrile and 14 mM NH_4HCO_3/acetic acid (pH 7.0). ESI–MS and NMR spectrometry were carried out for subsequent structural analyses of the purified reaction product. The mass spectrometer using LCT Premier XE (Waters) was operated in the negative mode with a cone voltage of −50 V. During the analysis, the mass spectrum was scanned from 100 to 400 $m\,z^{-1}$. For NMR analysis using an Inova500 (Varian), the purified product was lyophilized and dissolved in deuterium oxide. ^{1}H NMR and COSY spectra were monitored at a probe temperature of 25 °C with the solvent deuterium signal as an internal reference.

2.9. Crystallization and structure determination

The purified recombinant A1-R was concentrated (28.8 mg mL^{-1}) by ultrafiltration with a Centriprep centrifugal filter (Millipore). Commercial screening kits (Hampton Research, Emerald BioSystems, and Jena Bioscience) were used to search for the crystallization conditions of A1-R. The enzyme was crystallized by sitting-drop vapor diffusion on a 96-well Intelli-Plate (Varitas). The reservoir solution volume in each well was 100 μL, and the droplet was prepared by mixing 1 μL of the protein solution with 1 μL of the reservoir solution. A crystal of A1-R in complex with NADP (A1-R/NADP) was prepared in the solution containing NADP by cocrystallization.

Each crystal of A1-R and A1-R/NADP on nylon loop was placed directly in a cold nitrogen gas stream at −173 °C. X-ray diffraction images of the crystal were collected at −173 °C under the nitrogen gas stream with a Jupiter 210 CCD detector and synchrotron radiation of wavelength 1.0000 Å at the BL-38B1 station of SPring-8 (Hyogo, Japan). The distance between the crystal and detector was set to 150 mm, and 1° oscillation images were recorded with an exposure time of 4 s. Diffraction data for A1-R and A1-R/NADP were processed, merged, and scaled using the *HKL2000* program package (DENZO and SCALEPACK) [14]. The structure of A1-R was determined by molecular replacement with the *Molrep* program [15], supplied in the CCP4 program package [16] using coordinates of *Caenorhabditis elegans* glucose dehydrogenase (PDB ID, 1SPX) as an initial model. In the case of A1-R/NADP, molecular replacement was conducted using A1-R as an initial model. Structure refinement was conducted with the *Refmac5* program [17]. Randomly selected 5% reflections were excluded from refinement and used to calculate R_{free}. After each refinement cycle, the model was adjusted manually using the *Coot* program [18]. Water molecules were incorporated where the difference in density exceeded 3.0σ above the mean and the $2F_o - F_c$ map showed a density of over 1.0σ. Final model quality was checked with the *PROCHECK* program [19]. Protein models were superimposed and their root-mean-square deviation (r.m.s.d.) was determined with the *LSQKAB* program [20], part of CCP4. Coordinates used in this work were taken from the RCSB Protein Data Bank (PDB) [21]. Figures for the protein structure were prepared using the *PyMol* program [22].

2.10. Site-directed mutagenesis

To investigate the role of amino acid residues in A1-R, the enzyme mutants, except for a triple mutant G38D/R39E/K40E, were constructed using a QuikChange site-directed mutagenesis kit (Stratagene). The mutant G38D/R39E/K40E was constructed by using a KOD-Plus-Mutagenesis Kit (Toyobo), through an inverse PCR method. Plasmid pET21b/A1-R was used as a PCR template and oligonucleotides listed in Table 1 as primers. Mutations were confirmed by DNA sequencing with an automated DNA sequencer, as described earlier. Expression and purification of the mutants were performed using the same procedure as for the wild-type recombinant A1-R from *E. coli*.

2.11. Analytical procedures

SDS–PAGE was performed on a 12.5% polyacrylamide gel, as previously described [23]. Proteins in the gel were visualized by Coomassie Brilliant Blue R-250. The molecular mass of A1-R was estimated by native-PAGE. Native-PAGE was performed with a Native-PAGE Novex Bis–Tris gel system (Invitrogen), following the manufacturer's instructions. The products derived from DEH incubated with the strain A1 cell-free extract were separated by TLC using a solvent system consisting of 1-butanol, acetic acid, and water (3:2:2, vol./vol./vol.), and visualized by heating the TLC plate at 130 °C for 5 min after spraying it with 10% (vol./vol.) sulfuric acid in ethanol. Standard alginate disaccharides, with a molecular weight of 352, and trisaccharides, with a molecular weight of 528, were prepared by Bio-Gel P-2 column chromatography, as described previously [24]. The kinetic parameters (k_{cat} and K_m) for A1-R were calculated by using the Michaelis–Menten equation with Kaleida Graph (Synergy Software).

2.12. Data deposition

The nucleotide sequence of the A1-R gene reported in this paper has been deposited in the DDBJ, EMBL, and GenBank nucleotide sequence databases under GenBank ID: AB537450. The atomic coordinates and structure factors (PDB IDs: 3AFM for A1-R and 3AFN for A1-R/NADP) have been deposited in the Protein Data Bank,

Research Collaboratory for Structural Bioinformatics, Rutgers University, New Brunswick, NJ (http://www.rcsb.org/).

3. Results

3.1. DEH reductase activity in strain A1 cells

Extracts prepared from strain A1 cells grown on alginate were incubated with DEH in the presence or absence of various coenzymes. Reaction products were formed only in the presence of NADPH (Fig. 2a), indicating that an NADPH-dependent reductase, designated as A1-R, was responsible for the DEH metabolism.

The expression level of A1-R was examined in strain A1 cells grown on various carbon sources. A1-R activity was detected in the cells grown on all carbon sources tested, but the highest activity was found in the presence of alginate (Table 2).

Table 2
A1-R activity in strain A1 cells grown on different carbon sources.

Carbon source	Growth (OD_{600}[a])	Specific activity (U/mg)
Alginate	0.74	2.91
Pectin	0.71	0.023
Glucuronic acid	0.59	0.57
Glucose	0.54	0.26

All cells were cultured until late log phase.
[a] Optical density at 600 nm.

3.2. Enzymatic properties of A1-R

A1-R was purified 143-fold from strain A1 cells grown on alginate through seven steps of column chromatography, with a recovery of

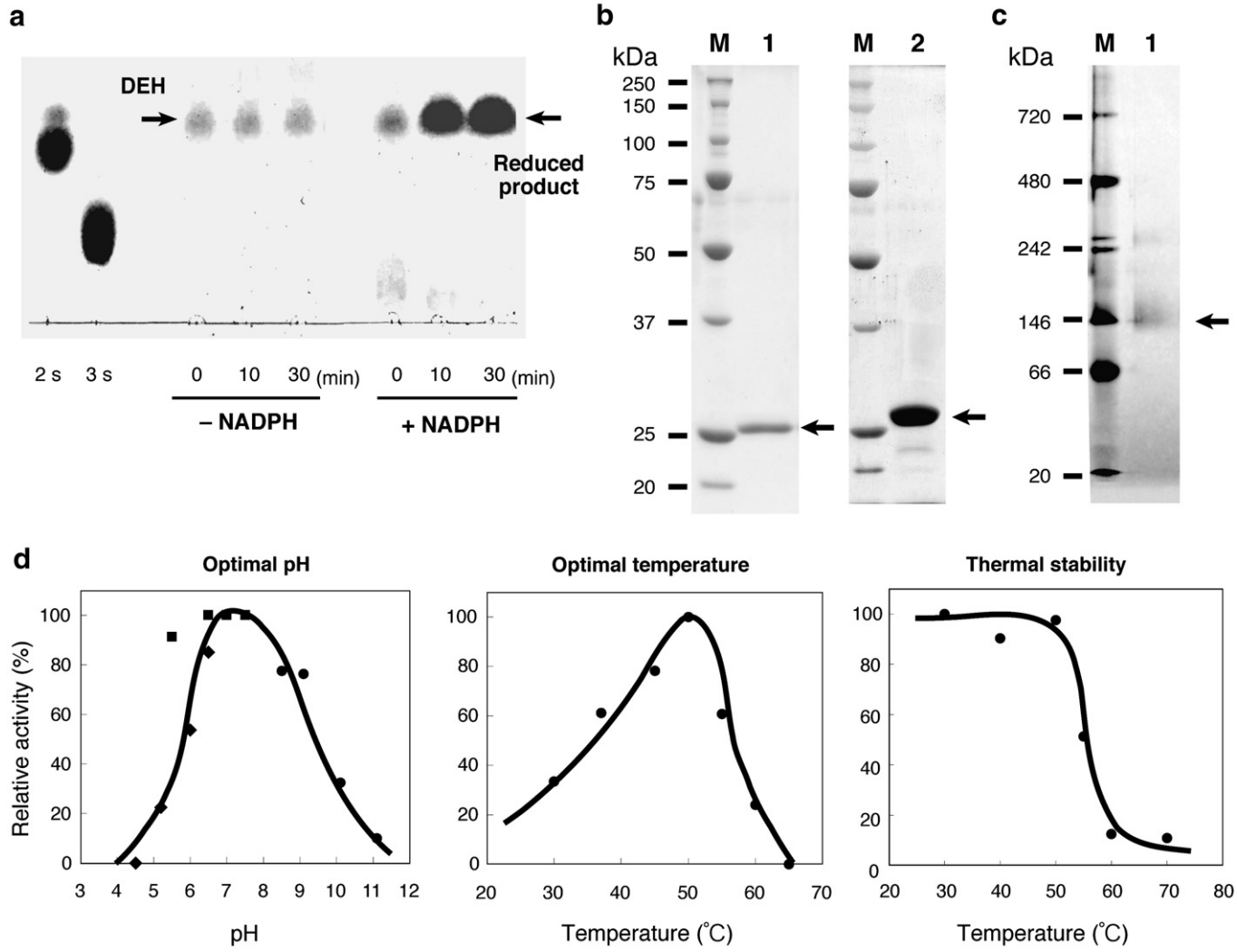

Fig. 2. Properties of A1-R. (a) DEH-reducing activity in the strain A1 cell-free extract. The reaction was performed at 30 °C in a reaction mixture consisting of 5 mg mL^{-1} DEH, 50 mM Tris–HCl (pH 7.5), 1 mM NADPH, and the appropriate amount of strain A1 cell-free extract. The reaction products were periodically sampled and analyzed on TLC plates, followed by staining with sulfuric acid. Alginate disaccharide (2 s) and trisaccharide (3 s) were used for marker control. (b) SDS–PAGE of purified A1-R followed by protein staining with Coomassie Brilliant Blue R-250. Lane M, molecular weight standards; lane 1, purified A1-R from strain A1 cells (1 μg of protein); lane 2, purified recombinant A1-R from *E. coli* cells (5 μg of protein). The arrow indicates the position of the enzyme. (c) Native-PAGE of purified A1-R followed by protein staining with Coomassie Brilliant Blue R-250. Lane M, molecular weight standards; lane 1, purified A1-R from strain A1 cells (5 μg of protein). The arrow indicates the position of the enzyme. (d) Effects of pH and temperature on the activity and stability of A1-R. Optimal pH (left): activity was assayed with sodium acetate (pH 4.5, 5.2, 6.0, and 6.5), KPB (pH 5.5, 6.5, 7.0, and 7.5), and glycine–NaOH (pH 8.5, 9.0, 10.0, and 11.0). Activity at pH 6.5–7.5 in KPB was taken as 100%. Optimal temperature (center): activity at 50 °C was taken as 100%. Thermal stability (right): the purified enzyme was preincubated for 5 min at various temperatures (as indicated) and the residual enzyme activity was measured. The activity of the enzyme preincubated at 4 °C for 5 min was taken as 100%.

Table 3
Purification of native A1-R from strain A1 and recombinant A1-R from *E. coli*.

Step[a]	Total protein (mg)	Total activity (U)	Specific activity (U mg^{-1})	Yield (%)	Purification (fold)
Native A1-R					
Cell-free extract	284	468	1.65	100	1.00
DEAE-Toyopearl 650 M	52.8	243	4.60	51.9	2.79
Q Sepharose HP	26.7	144	5.39	30.8	3.25
Superdex 75 pg	2.37	36.7	15.5	7.84	9.39
Hydroxylapatite	0.85	32.8	38.6	7.01	23.4
Butyl-Toyopearl 650 S	0.067	10.9	163	2.33	98.8
Superdex 200 pg	0.050	8.36	167	1.79	101
Mono Q	0.030	7.07	236	1.51	143
Recombinant A1-R					
Cell-free extract	2672	60.4	22.6	100	1.00
DEAE-Toyopearl 650 M	711	35.5	49.9	58.7	2.21
Butyl-Toyopearl 650 M	492	28.0	56.9	46.3	2.52

[a] The purification procedures are detailed in the Materials and methods.

1.51% (Table 3). The purified enzyme was homogeneous on SDS–PAGE analysis (Fig. 2b, left). The properties were as follows:

(i) Molecular weight. The molecular mass of A1-R was estimated to be 27 kDa through SDS–PAGE analysis (Fig. 2b, left). Native-PAGE analysis indicated A1-R was about 130 kDa (Fig. 2c), suggesting that, as is the case with the homologous protein [25], A1-R may be active in a tetrameric form. This is also supported by crystal structure of the enzyme as described below.

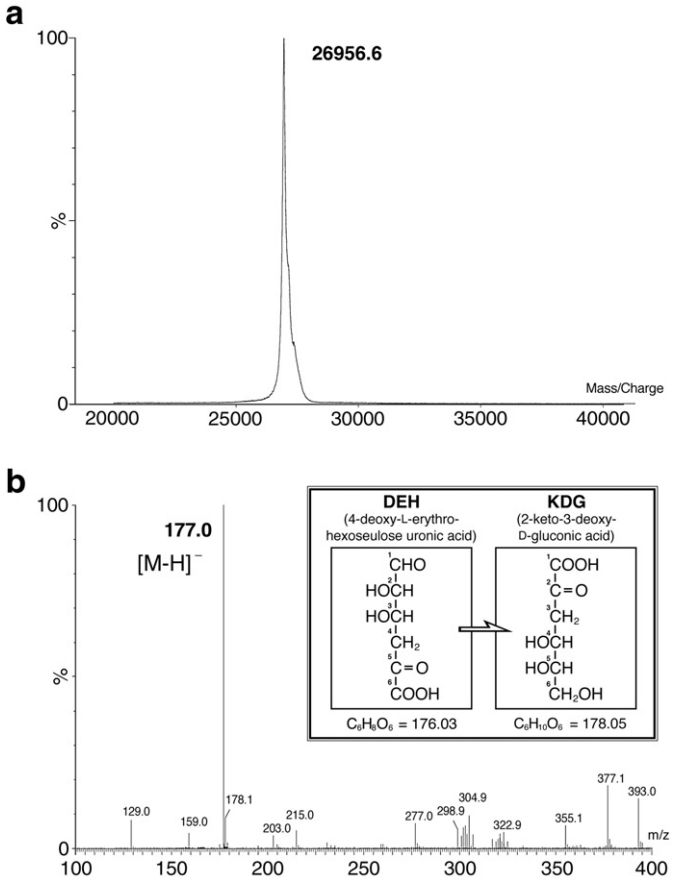

Fig. 3. MS. (a) MALDI–TOF–MS spectrum of A1-R. (b) ESI–MS spectrum of the reduced product from DEH through the A1-R reaction. The main peak in negative mode coincided with the molecular mass of the deprotonated form of DEH, namely KDG, indicated in the box.

Table 4
Kinetic parameters of recombinant wild-type and mutant A1-R for DEH.

Enzyme	k_{cat} (s^{-1})	K_m (mM)	k_{cat} K_m^{-1}	
			(mM^{-1} s^{-1})	(%)[a]
Wild-type	197 ± 8.9	1.93 ± 0.098	102	(100)
S150A	8.53 ± 0.25	16.2 ± 4.82	0.53	(0.52)
Y164F	0.129 ± 0.017	3.37 ± 0.78	0.038	(0.037)
K168A	35.2 ± 1.45	2.06 ± 0.17	17.1	(16.8)

[a] The k_{cat}/K_m value of the wild-type enzyme was taken as 100%.

(ii) Optimal pH and temperature. A1-R was the most active at pH 6.5–7.5 (KPB) and 50 °C, and stable below 50 °C (Fig. 2d). Replacement of KPB (pH 7.5) with Tris–HCl (pH 7.5) inhibited the activity (10–40%) of the enzyme (data not shown).
(iii) Chemicals. The reaction was conducted at 30 °C in the presence or absence of different compounds, and the residual activity was assayed (Supplementary Table 1S). About 65% of the enzymatic activity was lost in the presence of Hg^{2+} at 0.04 mM. Co^{2+} at 1 mM enhanced the enzymatic activity to 153%. Thiol reagents (dithiothreitol, glutathione (reduced form), 2-mercaptoethanol, iodoacetic acid, *p*-chloromercuribenzoic acid (1 mM)), a chelator of EDTA (1 mM), and sugars (L-fucose, D-galactose, D-glucose, D-mannose, L-rhamnose, D-xylose, D-sucrose, 2-deoxy glucose, D-glucosamine, D-glucuronic acid, D-galacturonic acid (5 mM)) had no effect (94–108%) on the reaction of A1-R.

Table 5
Statistics for X-ray diffraction and structure refinement.

	A1-R (native)	A1-R/NADP
Data collection		
Wavelength (Å)	1.0000	1.0000
Space group	$P3_221$	$P1$
Unit cell parameters (Å, °)	$a=b=106.2$, $c=70.4$	$a=60.4$, $b=64.2$, $c=74.4$ $\alpha=80.2$, $\beta=66.1$, $\gamma=65.0$
Resolution limit (Å)	50.0–1.65 (1.71–1.65)[a]	50.0–1.63 (1.69–1.63)[a]
Total reflections	840,225	287,719
Unique reflections	55,401	115,155
Redundancy	15.2 (14.3)	2.6 (2.4)
Completeness (%)	99.9 (99.8)	95.9 (88.8)
I/σ (I)	15.6 (4.99)	19.7 (3.82)
R_{merge} (%)	5.1 (40.1)	3.5 (17.2)
Refinement		
Final model	492 residues, 560 water molecules	1028 residues, 927 water molecules, 4 NADP molecules, 4 *tert*-butanol molecules
Resolution limit (Å)	31.2–1.65 (1.69–1.65)	22.7–1.63 (1.67–1.63)
Used reflections	52,496 (3796)	104,849 (6945)
Completeness (%)	99.9 (99.7)	95.9 (86.2)
R-factor (%)	17.6 (25.3)	17.2 (26.9)
R_{free} (%)	20.4 (31.0)	20.9 (31.7)
Average B-factor (Å^2)		
Protein		
Molecule A	15.6	17.3
Molecule B	16.2	17.3
Molecule C		18.9
Molecule D		19.0
Waters	30.4	32.6
NADP		
Molecule A		18.5
Molecule B		23.9
Molecule C		23.8
Molecule D		18.9
tert-butanol molecules		19.9
r.m.s.d.		
Bond (Å)	0.007	0.007
Angle (°)	0.96	1.06
Ramachandran plot (%)		
Favored regions	98.8	99.0
Allowed regions	100.0	100.0

[a] Data on highest shells is given in parenthesis.

(iv) Coenzyme and substrate specificity. A1-R was almost specific for NADPH and DEH (Supplementary Table 1S). Various ketones (4-methyl-2-pentanone, 2,5-hexanedione, and 3-chloropropiophenone), aldehydes (benzaldehyde, 4-methoxybenzaldehyde, *trans*-cinnamaldehyde), keto esters (ethyl pyruvate, ethyl benzoylacetate), and α-keto acid (sodium phenylpyruvate) were not utilized as substrates (data not shown). k_{cat} and K_m of A1-R were 274 s^{-1} and 101 μM towards DEH and 241 s^{-1} and 9.0 μM towards NADPH. A1-R was considered specific for NADPH rather than NADH since the enzyme activity in the presence of NADPH was 50-fold higher than that in the presence of NADH (Supplementary Table 1S).

3.3. Molecular identification of A1-R

The purified A1-R was subjected to peptide mass fingerprinting. After excision from the SDS–PAGE gel, the enzyme was digested with trypsin, and the resulting peptide fragments were used for subsequent LC-MS/MS and MS/MS ion search in the strain A1 genome database. The molecular masses of most fragments completely matched those of the partial amino acid sequence of SPH3227, with a sequence coverage of 47% (Supplementary Fig. 1S). SPH3227 is categorized into the "function-unknown protein family" in the strain A1 genome database. The protein consists of 258 amino acid residues with a theoretical molecular

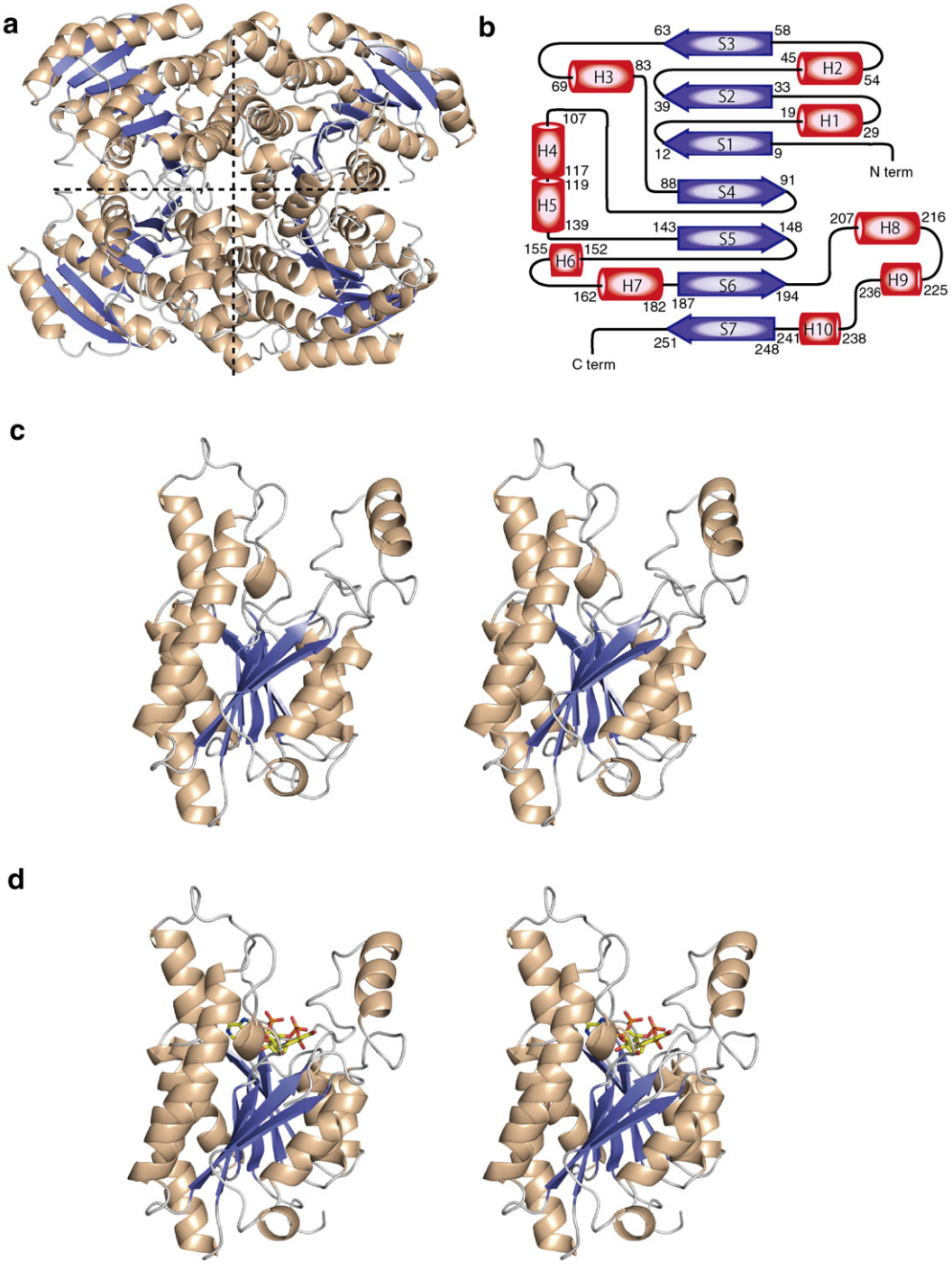

Fig. 4. Structure of A1-R. (a) Overall structure of A1-R in a biologically active tetramer form. (b) Topology diagram. β-Sheets are shown as blue arrows and α-helices as red cylinders. (c) Overall structure of A1-R in a monomeric form (stereodiagram). (d) Overall structure of A1-R/NADP in a monomeric form (stereodiagram). NADP is shown as a stick model.

weight of 26,931, which is in good agreement with that obtained from SDS–PAGE (27 kDa; Fig. 2b, left) and matrix-assisted laser desorption/ionization time-of-flight (MALDI-TOF)-MS (26,956.6 Da; Fig. 3a). These results indicated that SPH3227 is A1-R, an NADPH-dependent and DEH-specific reductase. Although the A1-R gene is located far from the genetic cluster for alginate import and degradation in the strain A1 genome, the A1-R gene is in the vicinity of the cluster of iron-related genes such as the outer membrane transporter for siderophore-iron complex and cytochrome. Since alginate is known to bind to iron, the transporter possibly incorporates iron using alginate as a siderophore. The cluster including the A1-R gene was also suggested related to alginate import and metabolism.

The sequence similarity analysis was carried out using the *BLAST* program on the GenomeNet server (http://blast.genome.jp). A1-R showed some sequence identity (15–35%) with most of the members of the short-chain dehydrogenase/reductase (SDR) superfamily, except for putative 3-ketoacyl-CoA reductase PhaB from *Vibrio splendidus* 12B01 (GenBank ID, AAMR01000010.1; 51.4% identity in 255-amino acid overlap) and a function-unknown protein from *Serratia proteamaculans* strain 568 (GenBank ID, CP000826; 51.4% identity in 255-amino acid overlap). Based on the primary structure, A1-R is also a member of the SDR superfamily. The subcellular localization prediction program *PSORTb* (http://www.psort.org/psortb/index.html) suggested that A1-R exclusively located in the cytoplasm as strain A1 alginate lyases responsible for depolymerization of alginate does.

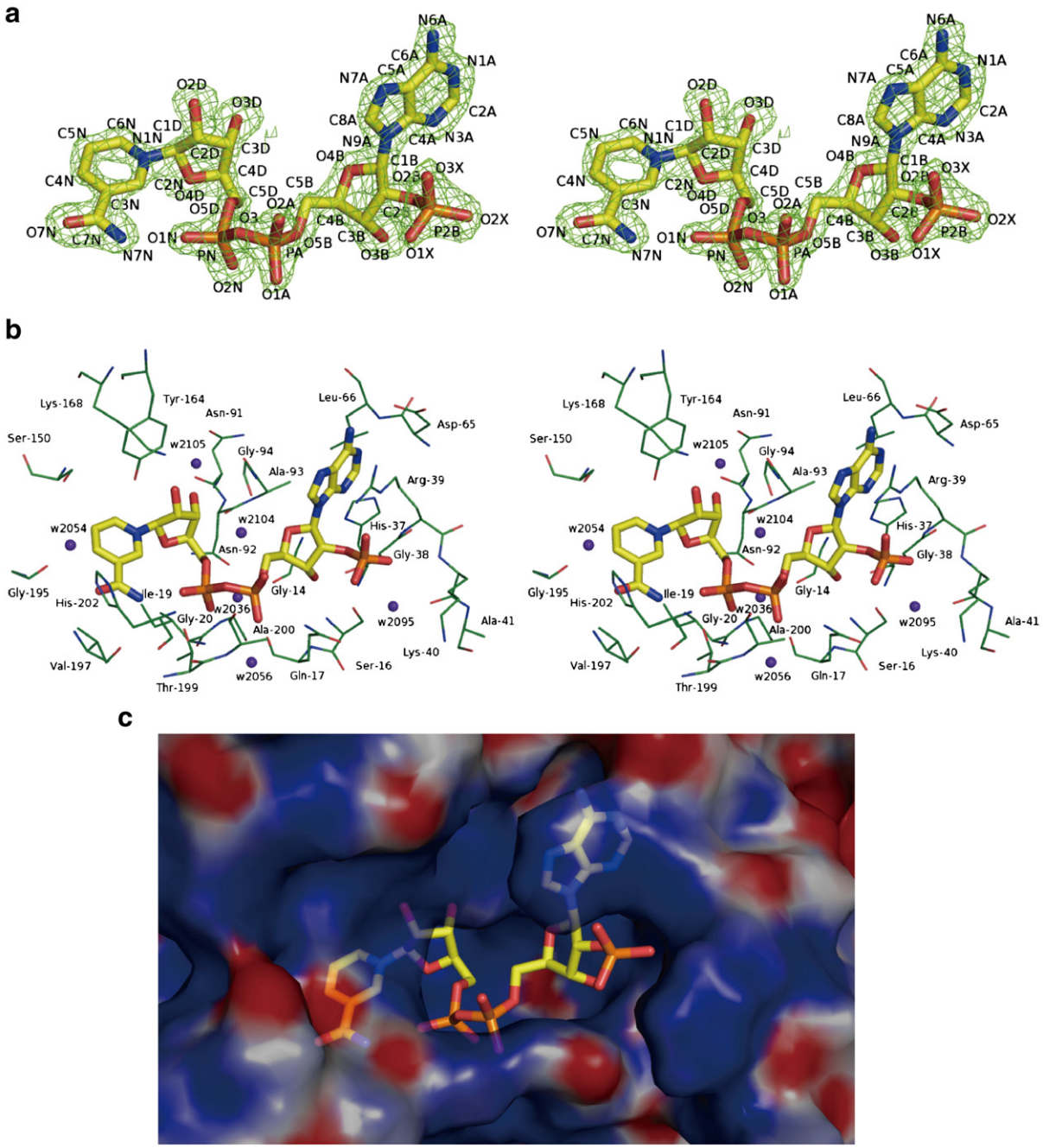

Fig. 5. Active site structure. (a) Electron density of NADP in the omit map ($F_o - F_c$), calculated at 3.0σ. (b) Residues interacting with NADP are shown by colored elements: carbon atom, green in residues and yellow in NADP; oxygen atom, red; nitrogen atom, blue; phosphate atom, orange. Purple balls represent water molecules. (c) Surface electrostatic potentials at pH 7.0 of the A1-R/NADP complex. Basic, blue; acidic, red.

3.4. Recombinant A1-R from E. coli cells

An overexpression system of A1-R was constructed in *E. coli* cells. Recombinant A1-R was purified 2.52-fold through two steps of column chromatography, with a recovery of 46.3% (Table 3). The purified enzyme was homogeneous by SDS–PAGE (Fig. 2b, right) and showed DEH-reducing activity. The N-terminal amino acid sequence of recombinant A1-R was ^{1}MFPDLK^{6}, indicating that no excision of the N-terminal amino acid residues occurred in the *E. coli* cells. This result coincided with the subcellular localization prediction (cytoplasm) of A1-R. The enzymatic properties of recombinant A1-R were similar to those of native A1-R from strain A1 cells, except for the specific activity (native A1-R, 236 U mg^{-1}; recombinant A1-R, 56.9 U mg^{-1}) and affinity to DEH (K_m for native A1-R, 101 μM; K_m for recombinant A1-R, 1930 μM) (Table 4). The difference in kinetic parameters between native and recombinant A1-Rs will be attributed to the inappropriate folding of A1-R in overexpression system.

3.5. Identification of the reaction product of A1-R

The reaction product of recombinant A1-R was purified and subjected to MS. In the ESI-MS spectrum (Fig. 3b), the major peak of deprotonated ion [M-H]$^-$ in negative mode indicated $m\ z^{-1}$ 177.0, demonstrating that the molecular weight of the product corresponded to that of the reduced form ($C_6H_{10}O_6$, MW = 178.05) derived from DEH ($C_6H_8O_6$, MW = 176.03). Furthermore, ^{1}H NMR and COSY spectra provided evidence that reduction of the aldehyde group at the 1-position carbon occurred in the A1-R product. These data revealed that A1-R catalyzed the reduction of DEH to KDG (Fig. 1).

3.6. Crystal structure of A1-R

To clarify the reaction mechanism of NADPH-dependent DEH reduction, X-ray crystallography of A1-R was conducted. An A1-R crystal was obtained in a reservoir solution consisting of 85 mM Tris–HCl (pH 8.4), 170 mM Li_2SO_4, 25.5% PEG4000, and 15% glycerol. The crystal structure of A1-R was determined at 1.65 Å resolution by the molecular replacement method, with an *R*-factor of 17.6% and a free *R*-factor of 20.4%. Data collection and refinement statistics are summarized in Table 5.

The refined model in an asymmetric unit consists of two identical monomers, termed molecules A and B. All the residues could be assigned in the $2F_o - F_c$ map of the molecule A, although residues 195-215 and 256-258 were absent in the $2F_o - F_c$ map of the molecule B. The r.m.s.d. between molecules A and B was calculated as 0.438 Å for all residues (228 Cα atoms). Because of the inclusion of almost all residues, molecule A is focused on hereafter. On the basis of theoretical curves in the plot, calculated according to the procedure of Luzzati [26], the absolute positional error was estimated to be 0.166 Å at a resolution of 1.65 Å. Ramachandran plot analysis [27], in which the stereochemical correctness of the backbone structure is indicated by (ϕ, ψ) torsion angles [28], shows that 98.8% of nonglycine residues lie within the favored regions and 100% of nonglycine residues lie in the allowed regions.

The overall structure and topology of the secondary structure elements indicate that A1-R consists of three-layered structure, α/β/α, with an coenzyme-binding Rossmann fold [29] (Fig. 4). The enzyme includes 10 α-helices (H1, residues 19–29; H2, residues 45–54; H3, residues 69–83; H4, residues 107–117; H5, residues 119–139; H6, residues 152–155; H7, residues 162–182; H8, residues 207–216; H9, residues 225–236; H10, residues 238–241) and 7 β-strands (S1, residues 9–12; S2, residues 33–39; S3, residues 58–63; S4, residues 88–91; S5, residues 143–148; S6, residues 187–194; S7, residues 248–251).

Structural homologues of A1-R were searched for in the PDB using the *Dali* program [30]. Several proteins included in the SDR superfamily, such as 3-oxoacyl reductase (PDB ID, 2UVD, $Z = 35.5$), were found to exhibit significant structural homology to A1-R (Supplementary Table 2S).

3.7. Coenzyme binding

To identify structural determinants for coenzyme binding, the A1-R/NADP crystal was obtained in the solution containing 500 μM NADP, 47% 2-methyl-2,4-pentanediol, and 2% *tert*-butanol by cocrystallization. The A1-R/NADP crystal belongs to space group *P*1 with unit cell parameters of $a = 60.4$Å, $b = 64.2$Å, and $c = 74.4$ Å ($\alpha = 80.2°$, $\beta = 66.1°$, $\gamma = 65.0°$). Four monomers, termed molecules A, B, C, and D, are present in an asymmetric unit. The initial phase was determined by molecular replacement with the ligand-free A1-R structure as the reference model. Only one N-terminal Met-1 could not be assigned in $2F_o - F_c$ maps of the four molecules. The r.m.s.d. between ligand-free A1-R and A1-R/NADP was calculated as 0.352 Å for all residues (246 Cα atoms); this indicates that no significant conformational change occurs between protein structures with and without NADP molecule.

NADP is accommodated in the Rossmann fold (Figs. 4d and 5). There are several hydrogen bond interactions between A1-R and NADP (Table 6). Direct and water-mediated hydrogen bonds are listed in Table 6. Arg-39 and Lys-40 form direct hydrogen bonds to the 2′-phosphate group of NADP, and N or O atom of NADP is directly bound to Gly-14, Ser-16, Gln-17, Ile-19, Asp-65, Leu-66, Asn-92, Tyr-164, Lys-168, Gly-195, Val-197, Thr-199, and His-202 via hydrogen bonds (Fig. 5b). In addition to hydrogen bond interactions, carbon–carbon contacts were also observed between the enzyme and NADP. Molecular surface electric charge at pH 7.0 was calculated using the

Table 6
Hydrogen bond (≤3.4 Å) between NADP, water molecules, and A1-R.

Direct interaction		Water-mediated interaction		
NADP atom	Protein/atom (distance, Å)[a]	NADP atom	Water (distance, Å)[b]	Protein/atom (distance, Å)[c]
Adenosine				
N1A	Leu-66/N (2.98)	O5B	Wat-2036 (3.17)	Gly-14/O (2.91)
N6A	Asp-65/OD1 (3.04)			Gln-17/O (2.89)
O3B	Gly-14/O (3.31)			Ile-19/N (3.31)
	Ser-16/OG (2.87)			Gly-20/N (2.83)
				Asn-92/OD1 (2.90)
Nicotinamide ribose				
O2D	Tyr-164/OH (2.71)	O3D	Wat-2105 (3.20)	Asn-91/O (2.97)
O3D	Lys-168/NZ (2.99)			Ala-93/O (2.95)
	Asn-92/O (2.78)			Lys-168/NZ (2.90)
O7N	Gly-195/O (3.31)	O7N	Wat-2054 (3.26)	Gly-195/O (2.73)
	Val-197/N (2.66)			His-202/NE2 (2.93)
	His-202/NE2 (2.90)			
N7N	Thr-199/OG1 (3.09)			
	Val-197/O (3.33)			
Diphosphate				
O1A	Gln-17/NE2 (2.81)	O1A	Wat-2056 (2.54)	Ala-200/N (2.92)
O1N	Thr-199/OG1 (2.64)	O2A	Wat-2104 (2.78)	Gly-94/O (3.04)
O2N	Ile-19/N (2.90)	O2N	Wat-2036 (2.69)	Gly-14/O (2.91)
				Gln-17/O (2.89)
				Ile-19/N (3.31)
				Gly-20/N (2.83)
				Asn-92/OD1 (2.90)
2′-Phosphate				
O2X	Arg-39/N (2.77)	O1X	Wat-2095 (3.21)	Ser-16/OG (2.74)
	Lys-40/N (3.22)			Lys-40/O (2.64)
O3X	Arg-39/NE (2.70)	O2X	Wat-2095 (2.63)	Ser-16/OG (2.74)
	Arg-39/NH2 (2.74)			Lys-40/O (2.64)

[a] Distance between the atom of NADP and protein.
[b] Distance between the atom of NADP and water.
[c] Distance between the atom of water and protein.

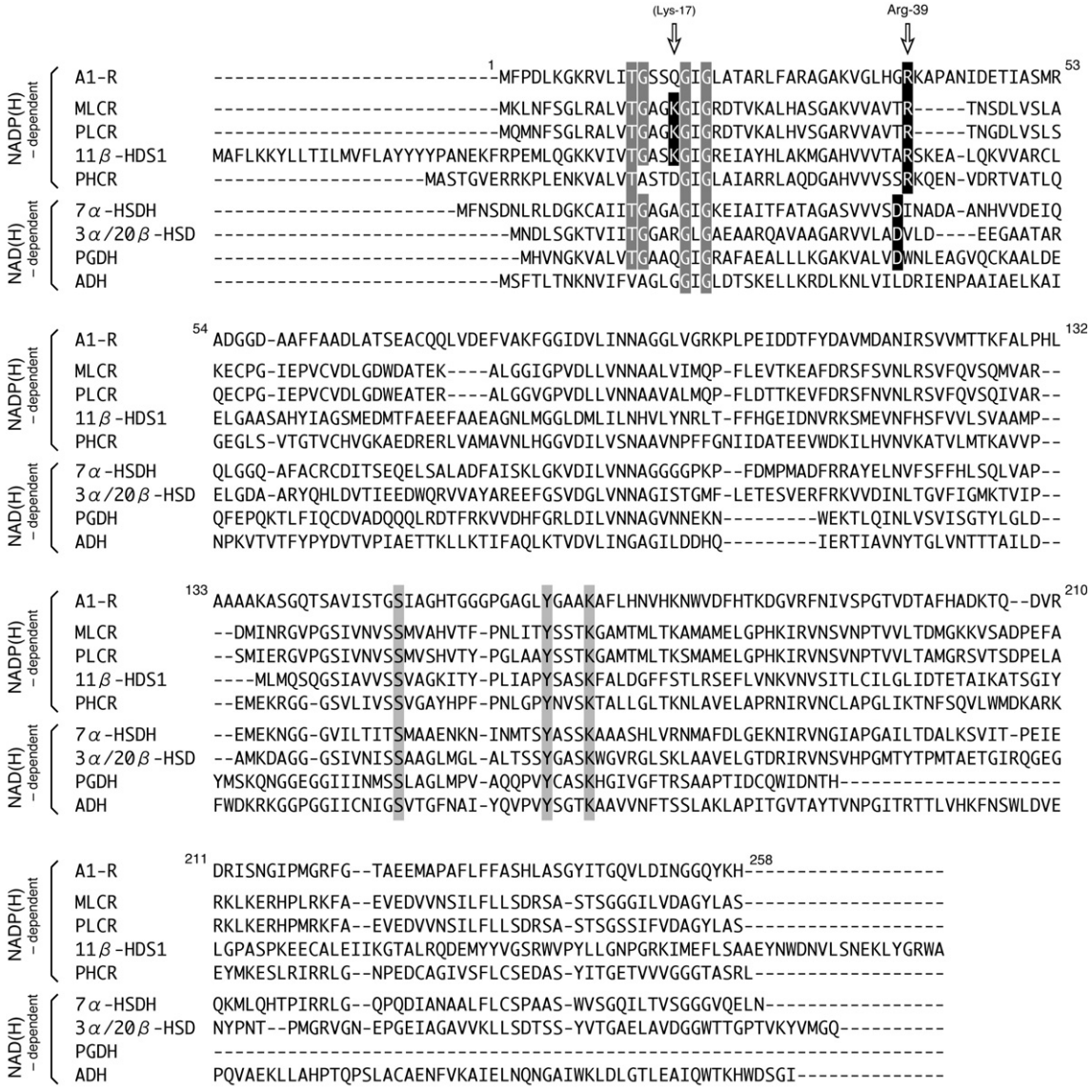

Fig. 6. Multiple sequence alignment of A1-R and well-known members of the SDR superfamily. MLCR (lung carbonyl reductase from *Mus musculus*, GenPept ID, Q542P5), PLCR (lung carbonyl reductase from *Sus scrofa*, GenPept ID, Q29529), 11β-HDS1 (11-β-hydroxysteroid dehydrogenase 1 from *Cavia porcellus*, GenPept ID, Q6QLL4), PHCR (heart carbonyl reductase from *Sus scrofa*, GenPept ID, Q8WNV7), 7α-HSDH (7-α-hydroxysteroid dehydrogenase from *E. coli*, GenPept ID, AAC74691), 3α/20β-HSD (3-α [or 20-β]-hydroxysteroid dehydrogenase from *Streptomyces exfoliates*, GenPept ID, P19992), PGDH (15-hydroxyprostaglandin dehydrogenase from *Homo sapiens*, GenPept ID, P15428), and ADH (alcohol dehydrogenase from *Drosophila melanogaster*, GenPept ID, P00334). The amino acid sequences were aligned by using ClustalW (http://clustalw.genome.jp/). The alignment indicates the cofactor-binding Thr-Gly-X-X-X-Gly-X-Gly motif (outlined characters on a shaded background) and catalytic triad Tyr-Lys-Ser (characters on a light-shaded background) within the enzymes. The residues involved in the specificity of NADP(H) or NAD(H) are shown as outlined characters on a black background.

APBS program (Fig. 5c). Positively charged residues, such as Arg-39 and Lys-40, form a basic pocket around the 2′-phosphate group of NADP, suggesting that the phosphate group is stabilized by this basic pocket.

A multiple sequence alignment of A1-R and some well-known members of the SDR superfamily is shown in Fig. 6. Arg-39 of A1-R was completely conserved among NADP(H)-dependent enzymes, while Asp was highly conserved among NAD(H)-dependent enzymes in place of Gly-38. In fact, Arg-39 is directly hydrogen bonded to the 2′-phosphate group of NADP (Fig. 5b and Table 6). To clarify the preference of A1-R for NADPH, 12 enzyme mutants were constructed through site-directed mutagenesis and subjected to the enzyme assay in the presence of NADPH (Table 7). The mutants in Gly-38 and Arg-39, such as G38D, R39I, R39V, and R39W, significantly decreased the affinity for NADPH, while there was little difference in the activity for NADH among the mutants.

3.8. Catalytic triad in A1-R

In the multiple sequence alignment (Fig. 6), SDR superfamily enzymes shared sequence identity of 18–32%, with highly conserved sequence motifs, such as the glycine-rich pattern of the cofactor-binding Rossmann fold region (Thr-Gly-X-X-X-Gly-X-Gly) [25,29,31] and catalytic triad (Tyr, Lys, and Ser) [25]. The conserved catalytic triad of A1-R corresponded to Ser-150, Tyr-164, and Lys-168. To confirm that these function as catalytic residues, we constructed A1-R mutants S150A, Y164F, and K168A, in which Ser-150, Tyr-164, and Lys-168 were replaced with Ala, Phe, and Ala, respectively. The mutants were purified and subjected to kinetic analysis (Table 4). All the mutants significantly reduced the enzymatic activity (k_{cat} K_m^{-1}). In particular, Y164F showed a significantly low k_{cat} value, suggesting that Tyr-164 may function as a proton donor in the reduction reaction. Ser-150 and Lys-168 may participate in catalysis by stabilizing the intermediates or in proton transfer, as described elsewhere [25,32].

Table 7
Kinetic parameters of wild-type and mutant A1-R proteins for NADPH and NADH.

Enzyme	NADPH				NADH			
	k_{cat} (s^{-1})	K_m (μM)	k_{cat} K_m^{-1}		k_{cat} (s^{-1})	K_m (μM)	k_{cat} K_m^{-1}	
			(mM^{-1} s^{-1})	(%)[a]			(mM^{-1} s^{-1})	(%)[a]
Wild-type	60.8 ± 3.6	7.01 ± 2.2	8700	(100)	7.59 ± 1.3	188 ± 55	40	(100)
G38D	5.16 ± 0.29	178 ± 17	29	(0.33)	8.29 ± 0.72	181 ± 28	46	(120)
R39I	7.80 ± 1.1	178 ± 43	44	(0.51)	10.6 ± 2.0	175 ± 59	60	(150)
R39V	16.2 ± 2.2	139 ± 21	120	(1.4)	10.2 ± 1.6	153 ± 25	66	(170)
R39W	2.13 ± 0.25	288 ± 48	7.4	(0.085)	9.86 ± 1.6	354 ± 84	28	(70)
A41E	81.7 ± 3.0	15.4 ± 2.3	5300	(61)	19.2 ± 5.1	402 ± 147	48	(120)
G38E	0.0767 ± 0.0041	282 ± 24	0.27	(0.0031)	0.270 ± 0.018	220 ± 22	1.2	(3.0)
R39D	0.108 ± 0.026	308 ± 105	0.35	(0.0040)	0.976 ± 0.18	227 ± 64	4.3	(11)
S16Y	3.59 ± 0.42	88.9 ± 21	40	(0.46)	0.546 ± 0.067	189 ± 37	2.9	(7.3)
G38D/R39E/K40E	N.D.	N.D.	N.D.	N.D.	N.D.	N.D.	N.D.	N.D.
G38D/R39D	N.D.	N.D.	N.D.	N.D.	0.0844 ± 0.028	557 ± 233	0.15	(0.38)
R39D/K40D	0.0618 ± 0.027	448 ± 255	0.14	(0.0016)	0.558 ± 0.17	446 ± 180	1.3	(3.3)
K40D/A41D	3.93 ± 0.48	78.0 ± 22	50	(0.57)	8.98 ± 2.4	160 ± 77	56	(140)

N.D., not determined due to low activity.
[a] The k_{cat}/K_m value of the wild-type enzyme was considered to be 100%.

4. Discussion

In this work, a novel bacterial aldose reductase was identified to catalyze the conversion of DEH to KDG. Judging from the data on KDG metabolism in bacteria [4], KDG formed from DEH in strain A1 cells is converted to 2-keto-3-deoxy-6-phospho-gluconic acid by 2-keto-3-deoxygluconokinase (A1-K), and then to D-glyceraldehdye-3-phosphate and pyruvate by 2-keto-3-deoxy-6-phospho-gluconate aldolase (A1-A; Fig. 1). Candidates for kinase A1-K (35 kDa) and aldolase A1-A (24 kDa) are included in the strain A1 genome database (data not shown). Although the involvement of an NADPH-dependent reductase, like A1-R, in alginate metabolism was reported in a certain pseudomonad in 1962 [4], little information on the molecular identification and physiological function of the enzyme has been accumulated. The A1-R gene was, therefore, first identified to encode the aldose reductase responsible for alginate metabolism. The enzymatic properties of A1-R were compared with those of the DEH reductase from the pseudomonad (designated PDEHR) [4]. A1-R and PDEHR are similar in terms of the optimal pH, behavior toward various compounds, and substrate specificity, but not susceptibility toward *p*-chloromercuribenzoic acid or affinity for DEH and NADPH.

On the basis of its primary and tertiary structures, A1-R is a member of the SDR superfamily, especially the "classical" SDR family [33]. The family members catalyze NAD(P)(H)-dependent redox reactions. They show a limited sequence identity (15–30%) throughout the entire molecules, although sequence motifs, such as the cofactor-binding Rossmann fold (Thr-Gly-X-X-X-Gly-X-Gly) [25,29,31] and catalytic triad (Tyr, Lys, and Ser) [25], are highly conserved. A1-R also shows some sequence identity 18–32% to the family members, but the catalytic triad formed by Ser-150, Tyr-164, and Lys-168 is well conserved in A1-R. These residues were found to be involved in the catalytic reaction of A1-R by site-directed mutagenesis and to constitute the catalytic triad around the cofactor-binding site by X-ray crystallography.

A glycine-rich pattern is also conserved in A1-R as Thr13-Gly14-X-X-X-Gly18-X-Gly20 (Fig. 6) and forms the classical βαβ motif of the Rossmann fold (Fig. 4), which facilitates NADPH binding. The specificity for NADP(H), rather than NAD(H), is believed to be conferred by two conserved basic residues in the Rossmann fold. In the mouse lung carbonyl reductase (MLCR), two basic residues, Lys-17 and Arg-34, have been suggested to promote NADPH binding by interacting with the 2′-phosphate group of NADP(H) [34,35]. Based on the sequence alignment, two basic residues in positions corresponding to Lys-17 and Arg-34 in the mouse reductase are conserved in almost all the members of the NADP(H)-dependent SDR superfamily but not in the NAD(H)-dependent members (Fig. 6). However, a single basic residue, Arg-39, alone is conserved in A1-R, as observed only rarely in the SDR superfamily members, such as NADP(H)-dependent pig heart carbonyl reductase (Fig. 6), suggesting that a specific binding motif for cofactor binding is included in A1-R. Site-directed mutagenesis studies indicate that Gly-38 and Arg-39 play important roles in NADPH binding. The mutant G38D showed no enhanced activity for NADH, suggesting that the preference for NADH in the SDR superfamily may be achieved by complex structural networks. Molecular conversion of A1-R with a preference for NADH requires a further structural study of A1-R in complex with NADH or substrate.

Acknowledgments

This work was supported by Promotion of Basic Research Activities for Innovative Bioscience (PROBRAIN) in Japan (to K.M.), Grants-in-Aid from the Japan Society for the Promotion of Science (to K.M. and W.H.), the Targeted Proteins Research Program of the Ministry of Education, Culture, Sports, Science, and Technology (MEXT) of Japan (to W.H.), and Research Fellowships from the Japan Society for the Promotion of Science for Young Scientists (to A.O.).

Appendix A. Supplementary data

Supplementary data associated with this article can be found, in the online version, at doi:10.1016/j.bbapap.2010.05.010.

References

[1] K. Murata, S. Kawai, B. Mikami, W. Hashimoto, Superchannel of bacteria: biological significance and new horizons, Biosci. Biotechnol. Biochem. 72 (2008) 265–277.
[2] H.-J. Yoon, W. Hashimoto, O. Miyake, M. Okamoto, B. Mikami, K. Murata, Overexpression in *Escherichia coli*, purification, and characterization of *Sphingomonas* sp. A1 alginate lyases, Protein Expr. Purif. 19 (2000) 84–90.
[3] W. Hashimoto, O. Miyake, K. Momma, S. Kawai, K. Murata, Molecular identification of oligoalginate lyase of *Sphingomonas* sp. strain A1 as one of the enzymes required for complete depolymerization of alginate, J. Bacteriol. 182 (2000) 4572–4577.
[4] J. Preiss, G. Ashwell, Alginic acid metabolism in bacteria: I. Enzymatic formation of unsaturated oligosaccharides and 4-deoxy-L-erythro-5-hexoseulose uronic acid, J. Biol. Chem. 237 (1962) 317–321.
[5] O. Miyake, W. Hashimoto, K. Murata, An exotype alginate lyase in *Sphingomonas* sp. A1: overexpression in *Escherichia coli*, purification, and characterization of alginate lyase IV (A1-IV), Protein Expr. Purif. 29 (2003) 33–41.
[6] A. Ochiai, W. Hashimoto, K. Murata, A biosystem for alginate metabolism in *Agrobacterium tumefaciens* strain C58: molecular identification of Atu3025 as an exotype family PL-15 alginate lyase, Res. Microbiol. 157 (2006) 642–649.
[7] F. Ausubel, R. Brent, R. Kingston, D. Moore, J. Seidman, J. Smith, K. Struhl, Current Protocols in Molecular Biology, John Wiley and Sons, New York, 1987.

[8] M.M. Bradford, A rapid and sensitive method for the quantitation of microgram quantities of protein utilizing the principle of protein–dye binding, Anal. Biochem. 72 (1976) 248–254.
[9] B. Thiede, W. Hohenwarter, A. Krah, J. Mattow, M. Schmid, F. Schmidt, P.R. Jungblut, Peptide mass fingerprinting, Methods 35 (2005) 237–247.
[10] W. Hashimoto, K. Momma, Y. Maruyama, M. Yamasaki, B. Mikami, K. Murata, Structure and function of bacterial super-biosystem responsible for import and depolymerization of macromolecules, Biosci. Biotechnol. Biochem. 69 (2005) 673–692.
[11] D.N. Perkins, D.J. Pappin, D.M. Creasy, J.S. Cottrell, Probability-based protein identification by searching sequence databases using mass spectrometry data, Electrophoresis 20 (1999) 3551–3567.
[12] F. Sanger, S. Nicklen, A.R. Coulson, DNA sequencing with chain-terminating inhibitors, Proc. Natl Acad. Sci. USA 74 (1977) 5463–5467.
[13] J. Sambrook, E.F. Fritsch, T. Maniatis, Molecular Cloning: A Laboratory Manual, Cold Spring Harbor Laboratory Press, Cold Spring Harbor, NY, 1989.
[14] Z. Otwinowski, W. Minor, Processing of X-ray diffraction data collected in oscillation mode, Meth. Enzymol. 276 (1997) 307–326.
[15] A. Vagin, A. Teplyakov, Molecular replacement with MOLREP, Acta Crystallogr. Sect. D. Biol. Crystallogr. 66 (2010) 22–25.
[16] Collaborative Computational Project, The CCP4 suite: programs for protein crystallography, Acta Crystallogr. Sect. D. Biol. Crystallogr. 50 (1994) 760–763.
[17] G.N. Murshudov, A.A. Vagin, E.J. Dodson, Refinement of macromolecular structures by the maximum-likelihood method, Acta Crystallogr. Sect. D. Biol. Crystallogr. 53 (1997) 240–255.
[18] P. Emsley, K. Cowtan, Coot: model-building tools for molecular graphics, Acta Crystallogr. Sect. D. Biol. Crystallogr. 60 (2004) 2126–2132.
[19] R.A. Laskowski, M.W. MacArthur, D.S. Moss, J.M. Thornton, PROCHECK: a program to check the stereochemical quality of protein structures, J. Appl. Crystallogr. 26 (1993) 283–291.
[20] W. Kabsch, A solution for the best rotation to relate two sets of vectors, Acta Crystallogr. Sect. A 32 (1976) 922–923.
[21] H.M. Berman, J. Westbrook, Z. Feng, G. Gilliland, T.N. Bhat, H. Weissig, I.N. Shindyalov, P.E. Bourne, The protein data bank, Nucleic Acids Res. 28 (2000) 235–242.
[22] W.L. DeLano, The PyMOL Molecular Graphics System, DeLano Scientific LLC, San Carlos, CA, 2004.
[23] U.K. Laemmli, Cleavage of structural proteins during the assembly of the head of bacteriophage T4, Nature 227 (1970) 680–685.
[24] W. Hashimoto, M. Okamoto, T. Hisano, K. Momma, K. Murata, *Sphingomonas* sp. A1 lyase active on both poly-β-D-mannuronate and heteropolymeric regions in alginate, J. Ferment. Bioeng. 86 (1998) 236–238.
[25] H. Jornvall, B. Persson, M. Krook, S. Atrian, R. Gonzalez-Duarte, J. Jeffery, D. Ghosh, Short-chain dehydrogenases/reductases (SDR), Biochemistry 34 (1995) 6003–6013.
[26] V. Luzzati, Traitement statistique des erreurs dans la determination des structures cristallines, Acta Crystallogr. 5 (1952) 802–810.
[27] S.C. Lovell, I.W. Davis III, W.B. Arendall, P.I.W. de Bakker, J.M. Word, M.G. Prisant, J.S. Richardson, D.C. Richardson, Structure validation by Cα geometry: ϕ, ψ and Cβ deviation, Proteins 50 (2003) 437–450.
[28] G.N. Ramachandran, V. Sasisekharan, Conformations of polypeptides and proteins, Adv. Protein Chem. 23 (1968) 283–438.
[29] M.G. Rossmann, D. Moras, K.W. Olsen, Chemical and biological evolution of nucleotide-binding protein, Nature 250 (1974) 194–199.
[30] L. Holm, S. Kääriäinen, P. Rosenstrom, A. Schenkel, Searching protein structure databases with DaliLite v.3, Bioinformatics 24 (2008) 2780–2781.
[31] H. Jornvall, M. Persson, J. Jeffery, Alcohol and polyol dehydrogenases are both divided into two protein types, and structural properties cross-relate the different enzyme activities within each type, Proc. Natl. Acad. Sci. U. S. A. 78 (1981) 4226–4230.
[32] N.S. Cols, S. Atrian, J. Benach, R. Ladenstein, R. Gonzalez-Duarte, Drosophila alcohol dehydrogenase: evaluation of Ser^{139} site-directed mutants, FEBS Lett. 413 (1997) 191–193.
[33] B. Persson, Y. Kallberg, U. Oppermann, H. Jörnvall, Coenzyme-based functional assignments of short-chain dehydrogenases/reductases (SDRs), Chem. Biol. Interact. 143–144 (2003) 271–278.
[34] M. Nakanishi, M. Kakumoto, K. Matsuura, Y. Deyashiki, N. Tanaka, T. Nonaka, Y. Mitsui, A. Hara, Involvement of two basic residues (Lys-17 and Arg-39) of mouse lung carbonyl reductase in NADP(H)-binding and fatty acid activation: site-directed mutagenesis and kinetic analyses, J. Biochem. (Tokyo) 120 (1996) 257–263.
[35] N. Tanaka, T. Nonaka, M. Nakanishi, Y. Deyashiki, A. Hara, Y. Mitsui, Crystal structure of the ternary complex of mouse lung carbonyl reductase at 1.8 Å resolution: the structural origin of coenzyme specificity in the short-chain dehydrogenase/reductase family, Structure 4 (1996) 33–45.